8-6-2021

Martensitic and inter-martensitic transformations in magnetocaloric Ni2.15Mn0.85Ga Heusler alloy

A. Madiligama
Penn State DuBois

P. Ari-Gur
Western Michigan University, pnina.ari-gur@wmich.edu

Y, Ren
X-ray Science Division, Argonne National Laboratory

V, Shavrov
Kotelnikov Institute of Radio-engineering and Electronics of RAS

Y. Ge
Aalto University; VTT Technical Research Centre of Finland

See next page for additional authors

DRAFT of what was later published as: A. Madiligama *et al*., "Martensitic and inter-martensitic transformations in magnetocaloric Ni2.15Mn0.85Ga Heusler alloy," in *IEEE Transactions on Magnetics*, doi: 10.1109/TMAG.2021.3102948.

Martensitic and inter-martensitic transformations in magnetocaloric $Ni_{2.15}Mn_{0.85}Ga$ Heusler alloy

A. Madiligama[1], P. Ari-Gur [2], Y. Ren[3], V. Shavrov[4], Y. Ge[5,6], J. George[7], I. Musabirov[8], V. Koledov[4,9]
[1]Penn State DuBois, DuBois, PA 15801, USA
[2]Department of Mechanical and Aerospace Engineering, Western Michigan University, Kalamazoo, MI 49008, USA
[3]X-ray Science Division, Argonne National Laboratory, Argonne, IL 60439, USA
[4]Kotelnikov Institute of Radio-engineering and Electronics of RAS, Moscow, 125009, Russia
[5]Aalto University, 02150, Espoo, Finland
[6]VTT Technical Research Centre of Finland, 02044, Espoo, Finland
[7]Department of Biomedical Engineering, University of Michigan, Ann Arbor, MI 48109, USA
[8]Institute for Metals Superplasticity Problems of Russian Academy of Sciences, Ufa, Stephan Khalturin str. 39, 450001, Russia
[9]Sirius University of Science and Technology, 1 Olympic Ave, 354340, Sochi, Russia

The entropy changes of successive martensitic phase transformations in Ni-Mn-Ga Heusler alloys can be utilized to realize enhanced magnetocaloric properties. A detailed study of phase transformations of one such alloy, $Ni_{2.15}Mn_{0.85}Ga$, (ΔQ = 4900 J/kg at 343 K, under 140 kOe), is reported here. Upon cooling, the paramagnetic cubic ($L2_1$) austenitic phase transforms into a ferromagnetic 7M modulated monoclinic martensitic phase. This phase is stable in a narrow temperature range, and upon further cooling, transforms into a non-modulated ferromagnetic tetragonal ($L1_0$) phase. The separation between the equilibrium temperatures of the austenitic and tetragonal martensitic phases is only ~50 K. The alloy undergoes reversible temperature-induced martensitic and inter-martensitic phase transformations with thermal hysteresis of about 25 K. The conclusions from the detailed study of the phase transformations lead to new possibilities to enhance the magnetocaloric effect by utilizing the entropy associated with multi-structural transformations.

Keywords: Multi-Structural Transformations, Ni-Mn-Ga Heusler Alloys, Thermal hysteresis

I. Introduction

One proposed solution to the low-efficiency and eco-adverse effects of current cooling technologies is magnetic cooling based on the giant magnetocaloric effect (MCE). It is considered as the approach with the best prospects to compete successfully with the current vapor-compression refrigeration technology [1]. The development of a magnetic material that produces a very large MCE near room temperature is a key to realizing efficient and economical magnetic cooling technology. Among the many novel magnetic materials that exhibit large MCE, Ni-Mn-X alloys are under the spotlight [2]. The massive isothermal entropy changes exhibited by some Ni-Mn-X alloys are close to the materials based on La-Fe-Si and Mn-Fe-P [3]. Therefore, Ni-Mn based Heusler alloys are considered as a promising contender for magnetic cooling applications [4].

Due to the strongest magneto-crystalline anisotropy in a single martensitic variant of single crystalline Ni-Mn-Ga alloys, they exhibit large inverse MCE under moderate magnetdic fields [5]. Nevertheless, these alloys are not practical for commercial cooling applications due to single crystals' high fabrication cost and processing complexities. In polycrystalline $Ni_{2.18}Mn_{0.82}Ga$ alloy, a more considerable entropy-change of 20.7±1.5 J/K kg under a magnetic field of H=1.8 T has been reported at the alloy's magneto-structural phase transformation temperature of 333.2 K [6]. Annealed $Ni_{2.08}Mn_{1.04}Ga_{0.88}$ melt-spun ribbons, with fine microstructure, were reported as exhibiting magnetocaloric entropy change of -30.0 J/K kg under 5 T thanks to the presence of magneto-multi-structural transitions [7]. It should be noted that in addition to the large magnetocaloric effect, Ni-Mn-X based ferromagnetic shape memory Heusler alloys draw considerable interest because of their other potential technological applications such as magnetoresistance [8], magnetic shape memory effect [9], and superelasticity [10]. The multifunctional nature of these alloys is expected to result in low-cost manufacturing of them in the future and will become even less expensive.

Stoichiometric Ni_2MnGa alloy undergoes two phase transformations: second-order phase transformation at Curie temperature (T_C) ~ 376 K from paramagnetic to ferromagnetic phase and a first-order structural

transformation at the martensitic transformation temperature (T_M) ~ 202 K from the $L2_1$ cubic phase to tetragonal martensitic phase [11]. Both transformation temperatures, T_C and T_M, of Ni-Mn-Ga alloys are very sensitive to the alloy's chemical composition [12]. T_M increases and T_C decreases with partial substitution of Mn with Ni in $Ni_{2+X}Mn_{1-X}Ga$ alloys, and the two transformations merge at X = 0.18 [13]. In addition to the magnetic and martensitic phase transformations (MT), Ni-Mn-Ga alloys undergo an inter-martensitic transformation (IMT), usually at low temperatures [14], [15]. By fine-tuning the chemical composition, MT and IMT can be brought closer and have two successive first-order phase transformations [16], [17]. Several techniques have been proposed to enhance the magnetocaloric effect demonstrated by Ni-Mn-X alloys. The latest trend is an enhanced MCE by utilizing the large isothermal entropy change that results from two successive martensitic phase transformations in Ni-rich Ni-Mn-Ga alloys [16], [17].

Here we report a comprehensive study of the MT and IMT phase transformations of one such $Ni_{2+X}Mn_{1-X}Ga$ alloy. The detailed analysis of the crystalline structures of the three phases, their phase transformation temperatures, and the thermal hysteresis will support the search for new avenues to enhance the magnetocaloric effect by utilizing the entropy associated with multi-structural transformations.

II. Experimental

A polycrystalline sample of Ni-Mn-Ga alloy was prepared by the arc-melting method in an argon atmosphere and annealed at 1073 K for 50 hours [6]. The chemical composition was determined by energy dispersive spectroscopy (EDS) analysis at Aalto University, Finland. The quantitative analysis was performed using standards of the elements present in the specimen (i.e., *Ni*, *Mn*, and *Ga*). The chemical composition of the alloy was found to be $Ni_{2.15}Mn_{0.85}Ga$, i.e., with excess *Ni* and deficiency of *Mn* compared to the stoichiometric Ni_2MnGa alloy. In-situ synchrotron diffraction data of polycrystalline samples were collected at beamline 11-ID-C of the Advanced Photon Source at Argonne National Laboratory (λ = 0.010804 nm). Small pieces of the samples (1 mm x 1 mm x 1 mm) were placed in a clear plastic tube (diameter ~ 3 mm and length ~ 20 mm), fastened to the sample holder. Although a powdered sample would have provided a better-quality diffraction pattern, the sample was not crushed to prevent deformation-induced phase transformations during the sample preparation process. The sample holder was rotated during the data collection process for better statistics. Data were collected as a function of temperature in the range 100-400 K while heating and then cooling in steps of 5 K. To determine the phase transformations, crystalline structures, and site occupancies of the alloys, Rietveld refinements of the synchrotron data collected at some selected temperature steps were carried out using General Structure Analysis System (GSAS) [18] and GSAS EXPGUI [19]. These schematic diagrams of the refined structures were generated by DRAWxtl [20], a software used in conjunction with GSAS to visualize the refined crystalline structures. Magnetization measurements of the sample were carried out as a function of both temperature (200-360 K) and magnetic field (0-4 T) using a SQUID magnetometer at the University of Michigan.

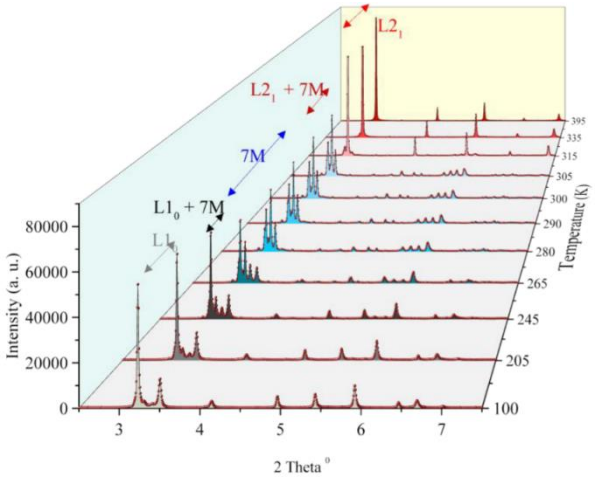

Fig. 1. Sample's diffraction data at selected temperatures (400-100K). These diffraction patterns were classified in to five groups.

DRAFT of what was later published as: A. Madiligama *et al*., "Martensitic and inter-martensitic transformations in magnetocaloric Ni2.15Mn0.85Ga Heusler alloy," in *IEEE Transactions on Magnetics*, doi: 10.1109/TMAG.2021.3102948.

III. RESULTS AND DISCUSSION

The observed diffraction patterns of this alloy in the temperature range 395 K to 100 K are shown in Fig. 1. They can be categorized into five groups, as summarized in Table 1. Starting from 395 K and down to around 340 K, the first category of diffraction patterns was identified as the austenitic phase. The second region from 340 down to 325 is a mixture of austenite and intermediate modulated martensitic phases. Pure intermediate modulated monoclinic phase is present only in a very narrow temperature range from 325 to 315. Below ~315 K and down to ~ 200 K, it is a mixture of two martensitic phases. Around 200 K and below, the observed diffraction pattern is entirely different from that of the rest of the temperature region. This diffraction pattern has a smaller number of Bragg peaks compared to the intermediate martensitic diffraction pattern. However, when compared to the austenitic diffraction pattern, this low-temperature martensitic pattern is more complicated.

TABLE1
Phases of the alloy upon cooling in the temperature range of 400-100 K

Temperature (K)	Phase(s) present
400–340	Cubic $L2_1$
340-325	Cubic $L2_1$ + *7M* modulated monoclinic
325-315	*7M* modulated monoclinic
315-215	*7M* modulated monoclinic + Tetragonal $L1_0$
215-100	Tetragonal $L1_0$

The Rietveld refinements revealed that the austenitic crystalline structure is cubic $L2_1$ ($Fm\bar{3}m$ space group). Several constraints were imposed on the site occupancy refinements. According to the EDS analysis, the Ga composition of the alloy is 25%; consequently, all the regular Ga-sites (4b) were constrained to be occupied exclusively by Ga atoms. Because the alloy has excess Ni concentration compared to that of the stoichiometric Ni_2MnGa alloy, it was assumed, as a starting point for the refinements, that all the regular Ni-sites (8c) were occupied only by Ni atoms, with the rest, sharing the 4a sites with the Mn atoms, according to ratio calculated from the EDS composition results. During the martensitic phase transformation, which is diffusion-less, atoms keep their relative neighborhood unchanged. Consequently, utilizing the site occupancy data of the austenitic phase, those in the martensitic phase was determined using the relationship between the crystalline structures. Results of the site occupancy refinements are summarized in Table 2, and a schematic representation of the average site occupancies is given in Fig. 2.

TABLE 2
Summary of the site occupancy refinement of the austenitic phase and refinement's agreement factors

Atom	Percentage site occupancy (%)			Chemical composition	Agreement factors of refinements		
	4(a)	4(b)	8(c)		χ^2	R_{WP}	R_P
Ni	14.8	-	99.8				
Mn	85.2	-	0.2	$Ni_{2.15}Mn_{0.85}Ga$	0.9	5.2	3.6
Ga	-	100	-				

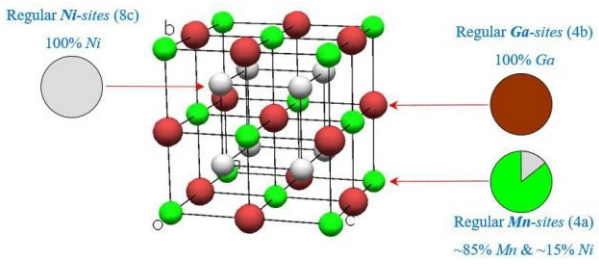

Fig. 2. A schematic representation of the average site occupancies of the cubic austenitic phase of the alloy.

The site occupancy refinement results were very close to the initial assumptions. The excess Ni atoms were found to occupy some of the regular Mn-sites (4a) and the Ga atoms occupy only their regular sites (4b). Almost all of the Mn atoms occupy their regular sites (4a) and only negligible amount was found in Ni-sites (8c). Calculated site occupancy results are in a good agreement with studies of the site occupancy refinement of neutron diffraction data of some Ni-Mn-Ga alloys with similar compositions, conducted independently by P. J. Lázpita et al. [21] and M. Barandiarán et al. [22].

The diffraction patterns collected at 320 K and 100 K without an applied magnetic field and compared with those calculated by the Rietveld refinements are shown in Fig. 3. At 320 K, the alloy is in the martensitic phase with 7M modulated monoclinic structure. This structure belongs to the $P\ 1\ 2/m\ 1$ space group. At 100 K, the alloy has completely transformed into the non-modulated martensitic phase. This structure is tetragonal and belongs to $I\ 4/m\ m\ m$ space group. The lattice parameters of all three structures (cubic, monoclinic, and tetragonal) are summarized in Table 3 with the agreement factor of the final refinement cycle in each phase.

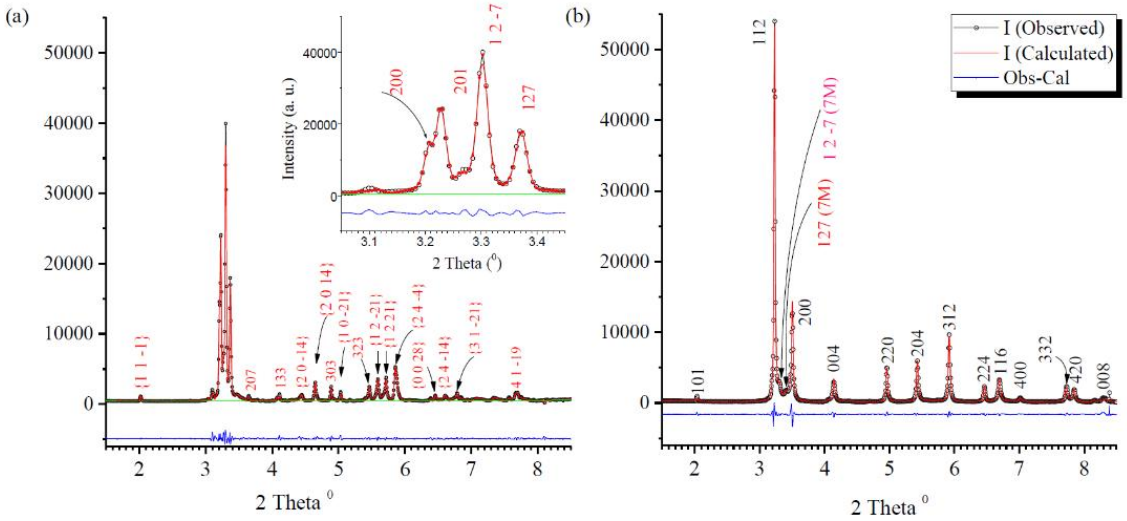

Fig. 3. Observed and calculated synchrotron diffraction patterns at (a) 320 K and (b) at 100 K under zero applied magnetic field. At 320 K, the alloy is in the inter-martensitic phase, which is a *7M* modulated structure. When the temperature goes down, this transforms in to the $L1_0$ tetragonal martensitic phase.

TABLE 3: Summary of the crystallographic information of the refined structures

Phase and crystalline structure	Experimental conditions	Lattice Parameters ($\alpha = \beta = 90.0^0$)				Stacking sequence (Zhdanov notation)	Space Group	Agreement factors		
		a (nm)	b (nm)	c (nm)	β (^{0})			R_{WP}^b	R_P^c	$\chi^{2\,d}$
Cubic $L2_1$	400 K/0 T	0.5812 (6)	-	-	90.0	-	$Fm\bar{3}m$	6.96	4.69	1.638
7M monoclinic	265 K/0T	0.4238(6)	0.5492(6)	2.936(6)	93.6	$\bar{2}5\bar{3}4$	$P\ 1\ 2/m\ 1$	6.31	4.19	4.998
Tetragonal $L1_0$	100 K/0T	0.3855(6)	-	0.6529(6)	90.0	-	$I\ 4/m\ m\ m$	5.75	3.81	3.684

Austenitic and martensitic phase fractions were calculated using the Rietveld refinements of their diffraction data collected during cooling and heating. The thermograms shown in Fig. 4 were constructed using the phase fraction of each phase at selected temperatures in the range of 100-400 K. Two first-order phase transformations, martensitic and inter-martensitic, could be identified while heating and then cooling the alloy. Upon cooling, the alloy undergoes forward martensitic transformation around 310 K from austenitic

$L2_1$ to 7M modulated martensite. Upon further cooling, at around 260 K, the inter-martensitic phase transformation occurs from the 7M monoclinic to tetragonal $L1_0$ phase. The reverse-phase transformations occur while heating, as shown in Fig. 4.

The characteristic temperatures of the austenitic (A_S, A_F) and martensitic (M_S, M_F) phase transformations were determined by the intersections of the lines obtained by extrapolating the linear parts of the thermograms of the cubic $L2_1$ phase (Fig. 5-a). In a similar fashion, the phase transformation temperatures of the inter-martensitic phase transformation ($T_{IM}H$, $T_{IM}C$) and temperatures of the phase transformation from the tetragonal $L1_0$ to the monoclinic phase (M_S, M_F) were determined (Fig. 5-b).

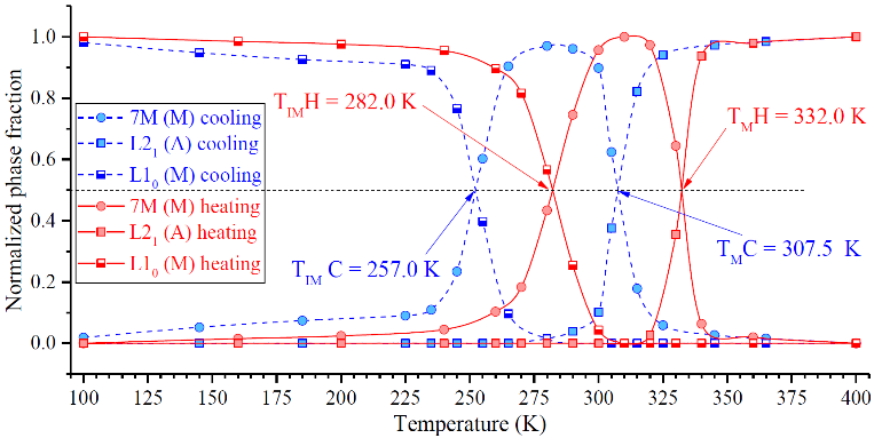

Fig. 4. Variation of the phase fractions of the three phases, cubic $L2_1$, 7M modulate monoclinic, and tetragonal $L1_0$, with temperature, upon heating (red) and cooling (blue), respectively.

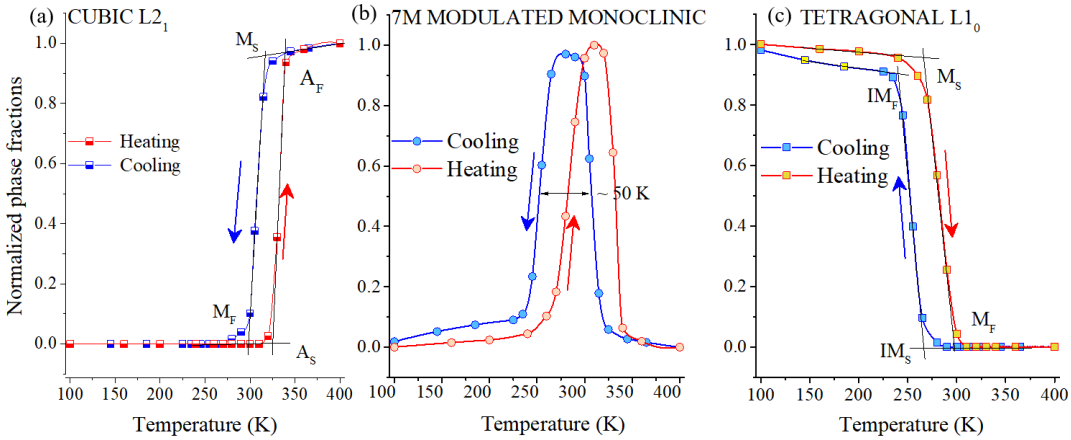

Fig. 5. Variation of the phase fractions of the (a) cubic, (b) 7M modulated monoclinic, and (c) tetragonal $L1_0$ phases with temperature upon heating (red) and cooling (blue). Characteristic temperatures of the martensitic and inter-martensitic phase transformations were determined by the intersections, as shown here.

Four additional temperatures, two for the martensitic phase transformation and two for the inter-martensitic phase transformation, were defined. T_MH and T_MC are the temperatures at which the phase fraction of the martensitic phase is half of the maximum value upon heating and cooling of the alloy, respectively. These values are taken as the martensitic phase transformation temperatures. $T_{IM}H$ and $T_{IM}C$ are the temperatures at which the phase fraction of the tetragonal $L1_0$ martensitic phase is half of the maximum value upon heating and cooling of the alloy, respectively. All these temperatures are summarized in Table 4. Thermal hystereses of martensitic and inter-martensitic phase transformations, calculated by taking the differences between T_MH & T_MC and between$T_{IM}H$ & $T_{IM}C$, respectively, are very close, ~25 K.

TABLE 4: *Characteristic temperatures and hysteresis of the martensitic and inter-martensitic phase transformations of the alloy*

Phase transformation	Characteristic temperatures of the phase transformations (K)						Hysteresis (K)
	A_S/ M_S	A_F/ M_F	M_S/ IM_S	M_F/IM_F	T_MC/ $T_{IM}C$	T_MH/ $T_{IM}H$	
Martensitic	330.0±0.5	346.0±0.5	322.0±0.5	301.0±0.5	307.5±0.5	332.0±0.5	24.5±0.7
Inter-martensitic	265.0±0.5	295.0±0.5	264.0±0.5	241.0±0.5	257.0±0.5	282.0±0.5	25.0±0.5

Fig. 6-a demonstrates the magnetic moment of the sample as a function of the temperature in the range 200-350 K under 50 Oe magnetic field. First the sample was zero-field cooled to 200 K and then field heated to 350 K and followed by field cooling back to 200 K. Upon field heating, the first magnetic phase transformation was observed around 312 K which is from ferromagnetic 2 to ferromagnetic 1. Upon further heating, a second transformation was observed at around 340 K from ferromagnetic 1 to paramagnetic. The reverse magnetic transformations occur almost at the same temperatures. The magnetic nature of the ferromagnetic phases 1 and 2 was confirmed by the mass magnetization vs. applied magnetic field measurements collected at 325 K (Fig. 6-b) and at 210 K (Fig. 6-c), respectively. In conclusion, the Curie temperature, T_C is around 340 K and the hysteresis is about 1K for both magnetic phase transformations.

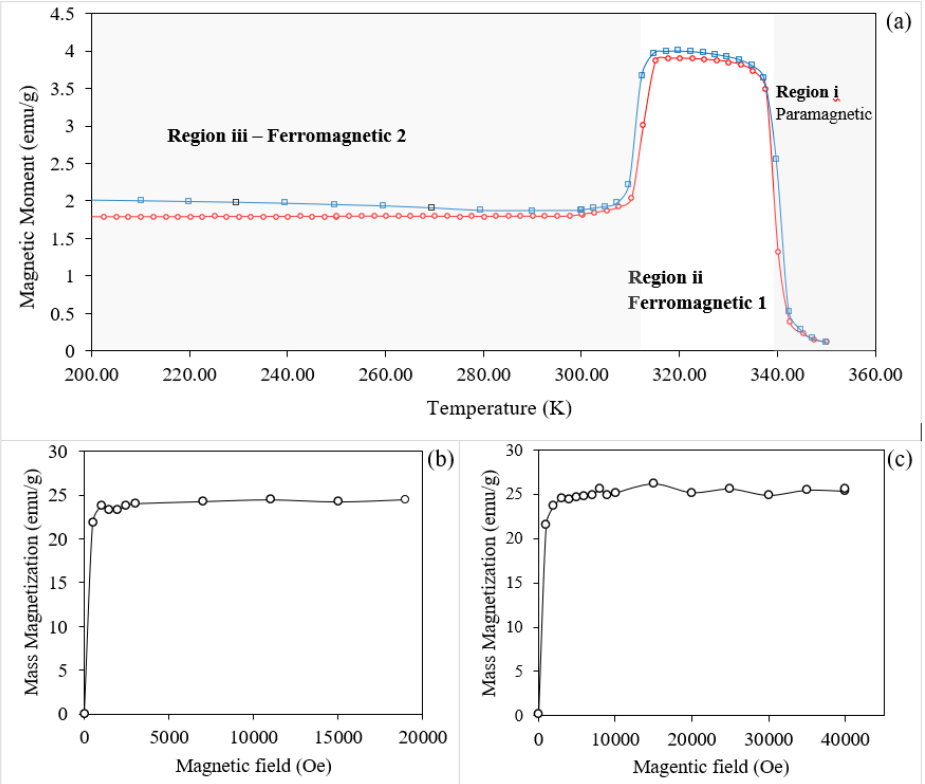

Figure 6: Magnetic measurements of the alloy. (a) Magnetization as a function of temperature under 50 Oe field heating and then cooling. (b) and (c) are the mass magnetization as a function of the applied magnetic field to the sample at 325 K and 210 K, respectively.

The crystalline phase transformation from 7M monoclinic to cubic phase is very close to the Curie temperature of 340 K. This indicates a coupled magnetostructural phase transformation from ferromagnetic 7M martensitic phase to cubic paramagnetic phase. The inter-martensitic phase transformation from tetragonal to 7M modulated monoclinic phase occurs upon heating to around 285 K. However, the second magnetic phase transformation between the two ferromagnetic phases occurs around 310 K and does not coincide with the inter-martensitic phase transformation. The mismatch between the second magnetic

transformation and inter-martensitic structural transformation temperatures is largely due to the high thermal hysteresis of the crystallographic phase transformations.

Compared with the martensitic phase transformation temperature, inter-martensitic phase transformations of some Ni-Mn-Ga alloys take place at much lower temperatures, resulting in a large temperature gap between the two phase-transformations. For example, V. A. Chernenko et al. [22] reported inter-martensitic phase transformations in Ni-Mn-Ga alloys at a temperature lower than the martensitic transformation by more than 100 K. The large separation between the two phase-transformations eliminates the possibility of enhancing the magnetocaloric effect by utilizing the entropy associated with multi-structural transformations. On the other hand, in the study of the $Ni_{2.15}Mn_{0.85}Ga$ alloy, the separation between the equilibrium temperatures of the two successive phase transformations is only about 50 K, and the hysteresis in both phase transformations are less than 25 K. Therefore, this alloy could be considered for use for enhanced magnetocaloric effect by utilizing the entropy associated with multi-structural phase transformations.

Phase transformation temperatures in Heusler alloys are sensitive to both magnetic field and even a small change of the chemical composition. In future studies, the effect of applied magnetic fields and compositional differences on both magnetic and crystallographic phase transformations, will be investigated. In addition, the composition will be changed, such as the addition of copper to reduce hysteresis [23].

IV. Conclusion

The studied $Ni_{2.15}Mn_{0.85}Ga$ alloy undergoes magneto-multi structural transitions with a narrow separation between the two successive phase transformations of only ~50 K and with hystereses of less than 25 K. All these conditions suggest that utilizing two successive phase transformations may result in higher Giant Magnetocaloric Effect (GMCE). To optimize the GMCE, extensive knowledge of two transformations is required. The magnetic phase transformation temperature increases with increasing magnetic field. However, the behavior of the crystalline phase transformation temperatures under different magnetic fields is unknown. The examination of the crystalline phase transformations under various magnetic fields is essential. Additionally, isothermal magnetization measurements could reveal the possible magnetic phase transformations.

Acknowledgment

This study was supported by Award No. RUP1-7028-MO-11 of the US Civilian Research and Development Foundation (CRDF Global) and by the National Science Foundation under Cooperative Agreement No. OISE-9531011. The authors also wish to acknowledge the US National Science Foundation award number NSF-0831951. Advanced Photon Source use was supported by the US Department of Energy, Office of Science, under contract No. DE-AC02-06CH1137. V. Shavrov is grateful for the support of the Russian Science Foundation Grant No. 20-19-00745. V. Koledov is grateful for the support of RFBR, Sirius University of Science and Technology, JSC Russian Railways, and Educational Fund “Talent and success,” project number 20-37-51005.

References

[1] D. R. Brown, N. Fernandez, J. A. Dirks, and T. B. Stout, "The prospects of alternatives to vapor compression technology for space cooling and food refrigeration applications," Prepared for the U.S. Department of Energy, under Contract DE-AC05-76RL01830 Report by Pacific Northwest National Laboratory, Washington, 2010.

[2] P. Lazpita, M. Sasmaz, J. M. Barandiaran, and V. A. Chernenko, "Effect of Fe doping and magneticfield on martensitic transformationof Mn-Ni(Fe)-Sn metamagnetic shape memory alloys," *Acta Mater.*, vol. 155, pp. 95-103, 2018.

[3] A. Waske, M. E. Gruner, T Gutfleisch, and O. Gutfleisch, "Magnetocaloric materials for refrigeration near room temperature," *MRS Bulletin*, vol. 43, pp. 269-273, 2018.

[4] Y. Qu, A. Gràcia-Condal, L. Mañosa, A. Planes, D. Cong, Z. Nie, Y. Ren and Y. Wang, "Outstanding caloric performances for energy-efficient multicaloric cooling in a Ni-Mn-based multifunctional alloy," *Acta Mater*., vol. 177, pp. 46-55, 2019.

[5] J. Marcos, L. Mañosa, A. Planes, F. Casanova, X. Batlle, and A. Labarta, "Multiscale origin of the magnetocaloric effect in Ni-Mn-Ga shape-memory alloys," *Phys. Rev. B*, vol. 68, p. 094401, 2003.

[6] A. A. Cherechukin, T. Takagi, M. Matsumoto, V. D. and Buchel'nikovc, "Magnetocaloric effect in $Ni_{2+x}Mn_{1-x}Ga$ Heusler alloys," *Phys. Lett. A*, vol. 326, pp. 146-151, 2004.

[7] Z. Li, Y. Zhang, C. F. Sánchez-Valdés, J. L. Sánchez Llamazares, C. Esling, Z. Xiang, and Z. and Liang, "Giant magnetocaloric effect in melt-spun Ni-Mn-Ga ribbons with magneto-multistructural transformation," *Appl. Phys. Lett.*, vol. 104, p. 044101, 2014.

[8] J. M. Barandiarán, V. A. Chernenko, P. Lázpita, J. Gutiérrez, and J. Feuchtwanger, "Effect of martensitic transformation and magnetic field on transport properties of Ni-Mn-Ga and Ni-Fe-Ga Heusler alloys," *Phys. Rev. B*, vol. 80, pp. 104404-1-104404-7, 2009.

DRAFT of what was later published as: A. Madiligama *et al*., "Martensitic and inter-martensitic transformations in magnetocaloric Ni2.15Mn0.85Ga Heusler alloy," in *IEEE Transactions on Magnetics*, doi: 10.1109/TMAG.2021.3102948.

[9] K. Ullakko, J. K. Haung, C. Kantner, R. C. O'Handley, and V. V. Kokorin, "Large magnetic-field-induced strains in Ni_2MnGa single crystals," *Appl. Phys. Lett.*, vol. 69, pp. 1966-1968, 1996.

[10] T. Krenke, E. Duman, M. Acet, E. F. Wassermann, X. Moya, L. Mañosa, A. Planes, E. Suard, and B. Ouladdiaf, "Magnetic superelasticity and inverse magnetocaloric effect in Ni-Mn-In," *Phys. Rev. B*, vol. 75, p. 104414, 2007.

[11] P. J. Webster, K. R. A. Ziebeck, S. L. Town, and M. S. Peak, "Magnetic order and phase transformation in Ni_2MnGa," *Philos. Mag. B*, vol. 49:3, pp. 295-310, 1984.

[12] F. Albertini, L. Pareti, A. Paoluzi, L. Morellon, P. A. Algarabel, M. R. Ibarra, and L. Raghi, "Composition and temperature dependence of the magnetocrystalline anisotropy in $Ni_{2+x}Mn_{1+y}Ga_{1+z}$ (x+y+z=0) Heusler alloys," *Appl. Phys. Lett.*, vol. 81, p. 4032, 2002.

[13] V. V. Khovaylo, V. D. Buchelnikov, R. Kainuma, V. V. Koledov, M. Ohtsuka, V. G. Shavrov, T. Takagi, S. V. Taskaev, and A. N. Vasiliev, "Phase transitions in $Ni_{2+x}Mn_{1-x}Ga$ with a high Ni excess," *Phys. Rev. B Condens. Matter*, vol. 72, p. 224408, 2006.

[14] W. H. Wang, G. H. Wu, J. L. Chen, S. X. Gao, and W. S. Zhan, "Intermartensitic transformation and magnetic-field-induced strain in $Ni_{52}Mn_{24.5}Ga_{23.5}$ single crystals," *Appl. Phys. Lett.*, vol. 79, p. 1148, 2001.

[15] A. Cakir, L. Righi, F. Albertini, M. Acet, M. Farle, and S. Akturk, "Extended investigation of intermartensitic transitions in Ni-Mn-Ga magnetic shape memory alloys: A detailed phase diagram determination," *J. Appl. Phys.*, vol. 114, p. 183912 , 2013.

[16] F. Hu, S. Wei, X. L. Z. He, K. Xu, Y. Cao, and Y. Kang, "Enhanced magnetocaloric effects driven by two successive magnetostructural transformations in $Ni_{55.5}Mn_{17.8}Ga_{26.7}$ alloy under hydrostatic," *Solid State Commun.*, vol. 300, p. 113691, 2019.

[17] Z. Li, K. Xu, Y. Zhang, C. Tao, D. Zheng, and C. Jing, "Two successive magneto-structural transformations and their relation to enhanced magnetocaloric effect for $Ni_{55.8}Mn_{18.1}Ga_{26.1}$ Heusler alloy," *Sci Rep*, vol. 5, p. 15143, 2015.

[18] A. Larson and R. Von Dreele, "General structure analysis system (GSAS)," Los Alamos National Laboratory Report LAUR, pp. 86-748, 2004.

[19] B. H. Toby, "EXPGUI, a graphical user interface for GSAS," *J. Appl. Cryst.*, vol. 34, pp. 210-213, 2001.

[20] L. Finger, M. Kroeker, and B. H. Toby, "DRAWxtl - A program to make ball-and-stick, or polyhedral crystal structure drawings", Washington, DC: Advanced Visual Systems, Inc., 2005.

[21] P. Lázpita, J. M. Barandiarán, J. Gutiérrez, J. Feuchtwanger, V. A. Chernenko, and M. L. Richard, "Magnetic moment and chemical order in off-stoichiometric Ni-Mn-Ga ferromagnetic shape memory alloys," *New J. Phys.*, vol. 13, p. 033039, 2011.

[22] J. M. Barandiarán, V. A. Chernenko, P. Lázpita, J. Gutiérrez, M. L. Fdez-Gubieda, and A. Kimura, "Neutron and synchrotron studies of structure and magnetism of Shape Memory Alloys," *J. Phys. Conf. Ser.*, vol. 663, p. 012014 , 2015.

[23] E. Stevens, K. Kimes, D. Salazar, A. Mostafaei, R. Rodriguez, A. A. Acierno, P. Lazpita, V. Chernenko, and M. Chmielusa, "Mastering a 1.2 K hysteresis for martensitic para-ferromagnetic partial transformation in Ni-Mn(Cu)-Ga magnetocaloric material via binde jet 3D printing," *Addit. Manuf.*, vol. 37, p. 101560 , 2021.